



UNIVERSITY OF LEEDS

This is a repository copy of *Carrier scattering approach to the origins of dark current in mid- and far-infrared (terahertz) quantum-well intersubband photodetectors (QWIPs)* .

White Rose Research Online URL for this paper:
<http://eprints.whiterose.ac.uk/710/>

Article:

Etteh, N.E.I. and Harrison, P. (2001) Carrier scattering approach to the origins of dark current in mid- and far-infrared (terahertz) quantum-well intersubband photodetectors (QWIPs). *IEEE Journal of Quantum Electronics*, 37 (5). pp. 672-675. ISSN 0018-9197

<https://doi.org/10.1109/3.918580>

Reuse

See Attached

Takedown

If you consider content in White Rose Research Online to be in breach of UK law, please notify us by emailing eprints@whiterose.ac.uk including the URL of the record and the reason for the withdrawal request.



eprints@whiterose.ac.uk
<https://eprints.whiterose.ac.uk/>

Carrier Scattering Approach to the Origins of Dark Current in Mid- and Far-Infrared (Terahertz) Quantum-Well Intersubband Photodetectors (QWIPs)

Nkaepe E. I. Etteh and Paul Harrison, *Senior Member, IEEE*

Abstract—A carrier scattering approach is taken in an analysis of the affect on the dark current of extending the operating wavelength of conventional bound to continuum quantum-well intersubband photodetectors. It is found that both the sequential tunneling and the thermionic emission contributions to the dark current increase as the wavelength of the detector is extended from the mid- to far-infrared. Dark current designs rules are derived.

Index Terms—Far-infrared, infrared, intersubband, quantum wells, QWIP, terahertz (THz).

I. INTRODUCTION

THE DARK current determines the signal-to-noise ratio of quantum-well infrared photodetectors (QWIPs), and therefore, minimizing it is an important design criteria for their construction. Whilst these devices have been demonstrated very successfully at mid-infrared wavelengths [1]–[7], the promise of new applications[8]–[10] at longer wavelengths in the far-infrared (300–30 μm) or terahertz (1–10 THz) region of the spectrum is providing impetus to extend their operating wavelength. Moving to longer wavelengths implies that the photon energy will be reduced; therefore, in conventional bound-continuum QWIPs (see Fig. 1), the electron energy level will be closer to the top of the quantum well (QW). In fact, the energy of the incoming photons ($h\nu \sim 4\text{--}41$ meV) may be of the order of the thermal broadening of the electron distribution ($kT \sim 6$ meV at 77 K and 25 meV at 300 K).

The three major contributors to the dark current are illustrated in Fig. 2. The first, sequential tunneling [Fig. 2(a)], is really electron scattering from states localized in one QW to the next. This scattering actually has to be mediated by a “third party,” such as a phonon or another electron. The second, field-induced emission is again scattering mediated by either a phonon or another charge carrier, but this time it is from states some way up the subband distribution. Although this reduces the “activation energy,” the number of carriers at these energies is smaller, making this process less likely (particularly at the modest electric field strengths considered in this work). The third and final contribution to the dark current is that of thermionic emission, simply

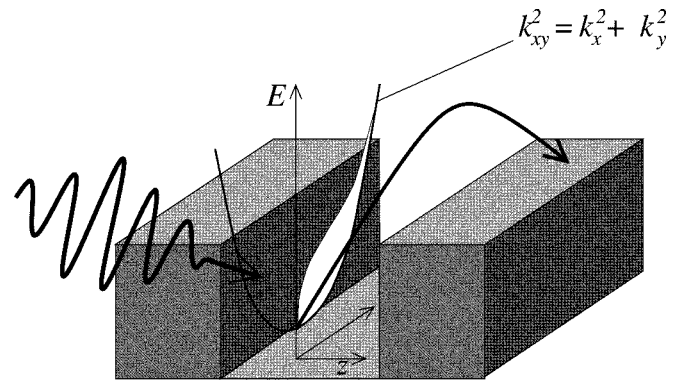


Fig. 1. Thermal broadening of the electron distribution in a QW subband can be of the same order as the photon energy in longer wavelength infrared detection.

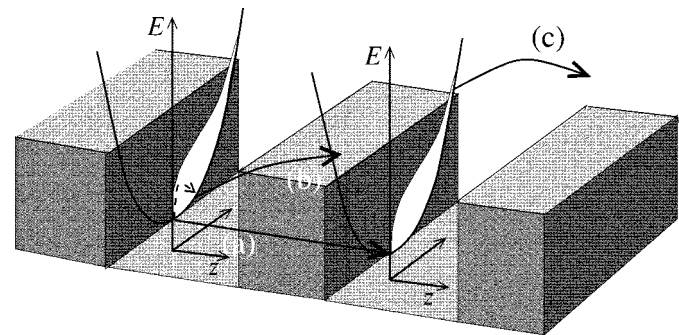


Fig. 2. Three possible mechanisms contributing to the dark current. (a) Sequential tunneling. (b) Field-induced emission. (c) Thermionic emission.

thermal excitation of the carriers directly out of the top of the QW and into continuum states above the semiconductor barriers where they are free to move and, hence, under the influence of the applied bias, constitute a current flow. All of the factors are influenced by the electron wave functions within the QWs constituting a QWIP and, indeed, as the QWIP is designed to work at longer and longer wavelengths, the electrons will be closer to the top of the QW and in turn all the above contributions to the dark current can be expected to increase.

Thus, the biggest challenge faced in designing and constructing long wavelength QWIPs is controlling the dark current. In this work, the affect of extending the operating wavelength, and other design parameters, on the dark current in conventional bound-continuum QWIPs will be evaluated using quantum mechanical carrier scattering.

Manuscript received July 24, 2000; revised January 25, 2001. This work was supported by the Institute of Microwaves and Photonics, the School of Electronic and Electrical Engineering, and The University of Leeds.

The authors are with the Institute of Microwaves and Photonics, School of Electronic and Electrical Engineering, University of Leeds, Leeds LS2 9JT, U.K. (e-mail: p.harrison@ee.leeds.ac.uk).

Publisher Item Identifier S 0018-9197(01)03482-0.

II. THEORETICAL APPROACH AND METHODS

The 1-D Schrödinger equation for an electron within a general semiconductor heterostructure, defined by the band-edge potential $V(z)$ under the envelope function/effective mass approximations and the influence of an electric field F , is

$$\left[-\frac{\hbar^2}{2} \frac{\partial}{\partial z} \frac{1}{m^*(z)} \frac{\partial}{\partial z} + V(z) - eFz \right] \psi(z) = E\psi(z) \quad (1)$$

where m^* is the effective mass of the electron and z is the distance along the growth axis. This was solved numerically using a shooting technique to generate both the energy eigenvalues E and the wave functions $\psi(z)$.

The resulting wave functions were used to calculate the electron-longitudinal optical (LO) phonon and electron-electron scattering rates using an approach based on Fermi's Golden Rule and the latter under the Born approximation (see Harrison [11] for full derivations and computer sourcecode). Thermalized electron distributions were assumed with the electron temperature taken equal to the lattice temperature.

III. THERMIONIC EMISSION

In the first instance, a simple model was constructed for evaluating the relative strength of the thermionic emission as a function of such parameters as detection wavelength and temperature. In particular, the strength of the thermionic emission process was taken as proportional to the density of electrons near the top of the well. The latter can be found simply by calculating the Fermi-Dirac distribution function of the subband electron population, the justification being that the electrons near the top of the QW are susceptible to ionization due to small energy scattering with other electrons and phonons, and hence, the more electrons in this situation, the more will be ionized.

Fig. 3 shows the results of calculations assuming a subband electron density of 10^{10} cm^{-2} . It can be seen that the contribution of thermionic emission to the dark current increases as the wavelength of the detector increases and as the temperature increases.

What is more important are the relative changes in this process with detection wave length. At temperatures of 100 K and above, the thermionic emission is two orders of magnitude higher within the far-infrared range at $40 \mu\text{m}$ than in the mid-infrared range at $10 \mu\text{m}$. QWIP-based cameras at the latter wavelengths already require cooling to 77 K [12], so it is quite clear that simply extending the wavelength using contemporary bound-continuum designs based on multiple-QWs will not be viable.

Improvements on this model would involve evaluating the scattering rates for electrons from within the QWs to the 3-D states above the barriers. At first sight, this is extremely complicated mathematically, as it involves evaluating scattering integrals over initial two-dimensional states into all final 3-D states. However, this can be achieved—although via somewhat intensive numerical calculations—by “discretising the continuum,” in effect turning the continuum into a series

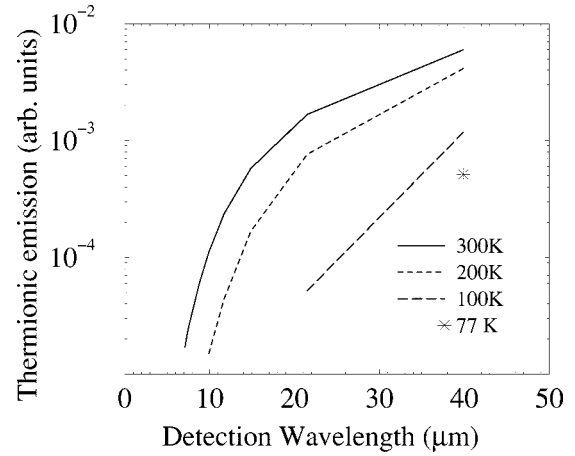


Fig. 3. Thermionic emission as a function of the detection wavelength for several different temperatures.

of closely spaced 2-D states and summing in the limit of an infinite number of states. It is not clear that this would give any further insights into understanding this process.

IV. SEQUENTIAL TUNNELLING

A. Suppression with Increased Barrier Width

Gunapala *et al.* [13] state that the contribution of sequential tunneling to the dark current can be reduced simply by increasing the width of the barrier separating adjacent QWs within the QWIP. Experimental observations of the dark current versus the barrier width in a series of otherwise identical QWIPs support this conclusion [14]. However, to the authors' knowledge a quantitative proof of this statement, based upon a carrier scattering approach, is not available in the literature, and this provides the motivation for this study. In addition, a theoretical approach—as here—allows a larger parameter space to be explored, and this will be exploited to investigate the relative strengths of sequential tunneling as the detection wavelength is increased.

Figs. 4 and 5 show the results of calculations of the electron-LO phonon and electron-electron scattering rates from the quantum confined subband in one well to the adjacent well, as a function of the detection wavelength and for several different barrier widths. Simple semiconductor theory gives the current density as $J = nqv$, where n is the density, q the charge and v the velocity of the carriers. In our model of a QWIP, the electrons scatter a distance equal to the period of the multiple-QW ($l_w + l_b$) in a time τ , where the latter is given by the scattering rate, i.e.,

$$\frac{1}{\tau} = \frac{1}{\tau_{\text{LO}}} + \frac{1}{\tau_{\text{ee}}}. \quad (2)$$

The velocity, therefore, follows as $v = (l_w + l_b)/\tau$. Thus, the higher any scattering rate $1/\tau_{\text{LO}}$ or $1/\tau_{\text{ee}}$, the larger the contribution of this mechanism to the dark current.

Examination of both Figs. 4 and 5, therefore, shows that the contribution of electron-LO phonon and electron-electron scattering to the sequential-tunneling component of the dark current increases with increasing detection wavelength. The (largely)

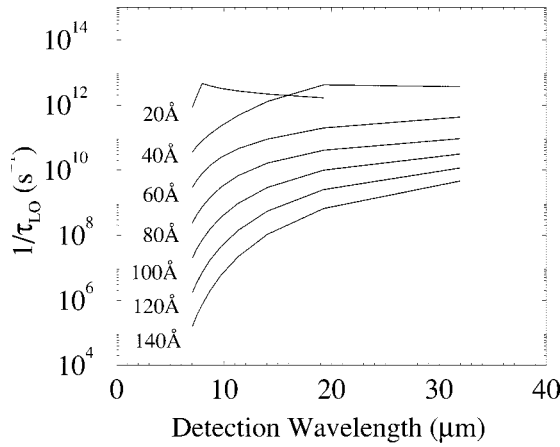


Fig. 4. Interwell electron-LO phonon scattering rate ($1/\tau_{LO}$) as a function of the barrier width (as indicated on the figure), at 77 K for an applied electric field of 10 kVcm^{-1} and thermalized electron distributions of $10 \times 10^{10} \text{ cm}^{-2}$ in each well.

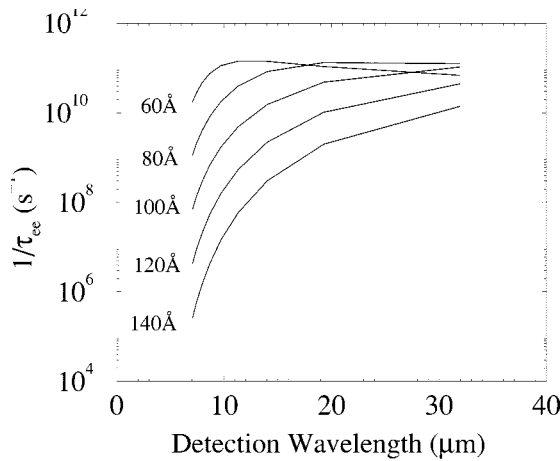


Fig. 5. Interwell electron-electron scattering rate ($1/\tau_{ee}$) as a function of the barrier width (as indicated on the figure), at 77 K for an applied electric field of 10 kVcm^{-1} and thermalized electron distributions of $10 \times 10^{10} \text{ cm}^{-2}$ in each well.

monotonic and uniform nature of the series of curves for different barrier widths suggests, for any given wavelength λ , an empirical relationship of the form

$$\frac{1}{\tau} = \alpha e^{-(l_b/\Lambda)} \quad (3)$$

for both electron-LO phonon and electron-electron scattering. Analysis shows that this is correct, with the constants given in Table I.

Examination of the data in Table I shows that as the detection wavelength increases from mid-to-far-infrared values the barrier required to reduce the sequential-tunneling component of the dark current also increases. This is due to the reduced *well* thickness pushing the electron states toward the top of the barrier, allowing the wavefunction to delocalize and overlap with the wavefunction in the adjacent wells. Thus, using standard QWIP designs and pushing them to longer wavelengths will require thicker barriers than their mid-infrared counterparts to keep the sequential tunneling to the same values.

TABLE I
SCATTERING RATES $1/\tau$ CAN BE EXPRESSED AS AN EMPIRICAL FUNCTION OF THE BARRIER WIDTH l_b AS IN (3), WITH THE DECAY CONSTANTS GIVEN FOR A RANGE OF DETECTION WAVELENGTHS λ

λ (μm)	Λ (\AA)	
	$1/\tau_{LO}$	$1/\tau_{ee}$
32.0	17.9	27.0
19.3	12.0	14.1
14.0	11.0	10.6
11.3	10.1	9.1
9.7	9.5	8.4
8.7	9.0	7.9
7.7	8.6	7.6
7.4	8.3	7.3
7.0	8.1	7.1

Besides this, the data in the table show that at wavelengths up to $20 \mu\text{m}$, the decay constants for both electron-LO phonon and electron-electron scattering mechanisms are very similar, i.e., an increase in barrier width l_b produces the same proportional decrease in both scattering channels. In addition, the rather small decay constants ($\lesssim 20 \text{ \AA}$) demonstrate that increasing the barrier width is an effective means of reducing the sequential-tunneling contribution to the dark current. The data in Table I compares well with the experimental measurements of Levine *et al.* [7], who observed a reduction in the dark current of four orders of magnitude when they increased the barrier width from 140 to 300 \AA (and simultaneously the barrier height) in a $\lambda = 8.3 \mu\text{m}$ QWIP. The data in the table covers this detection wavelength, and the correspondingly small decay constant of 9 \AA indicates that the sequential-tunneling contribution to the dark current will decay by many orders of magnitude when the barrier width is increased by 160 \AA , which is in line with the experimental observations.

Given a QWIP with a particular detection wavelength and measured dark current, this empirical relationship could be used to deduce the required barrier width to design the dark current to meet a specific requirement. For example, if a particular $9.7\text{-}\mu\text{m}$ QWIP design was found to have a dark current at its operating bias, and temperature of 1 nA , whereas the application required the dark current to be limited to 1 pA , then the data in Table I shows that for every ($\Delta =$) 9.5 \AA increase in the barrier width, the phonon sequential-tunneling contribution will be reduced by a factor of e^{-1} . To reduce this contribution by a factor of 10^{-3} implies that the barrier width must increase by an amount Δl_b , where

$$10^{-3} = e^{-(\Delta l_b/\Lambda)} \Rightarrow \Delta l_b = -\Lambda \ln(10^{-3}) \approx 66 \text{ \AA}. \quad (4)$$

B. Effect of Temperature

Under the models used in this work, the electron-electron scattering rate is a weak function of temperature (through both the changes in the screening term and the initial and final state distribution functions, see Harrison [11, p. 283]), and hence, makes a very small contribution to the effect of temperature on the sequential-tunneling rate. However, the electron-LO phonon scattering rate is strongly dependent upon temperature,

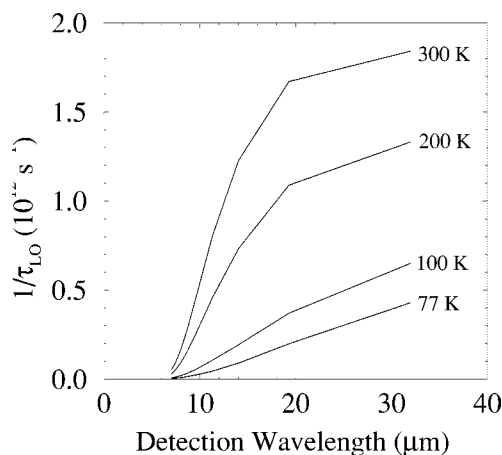


Fig. 6. Interwell electron-LO phonon scattering rate ($1/\tau_{LO}$) as a function of detection wavelength for several different temperatures, for an applied electric field of 10 kVcm^{-1} and thermalized electron distributions of $10 \times 10^{10} \text{ cm}^{-2}$ in each well, with $l_b = 60 \text{ \AA}$.

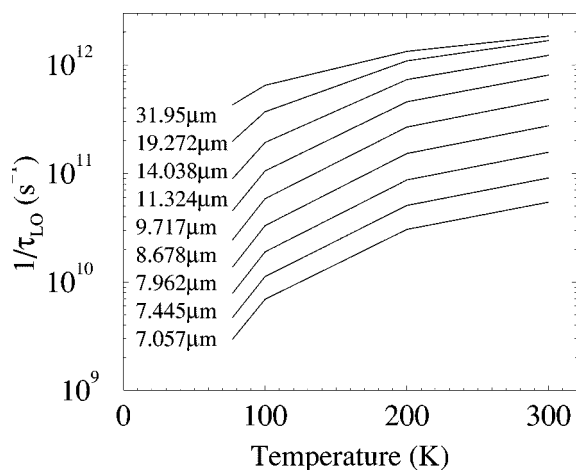


Fig. 7. Interwell electron-LO phonon scattering rate ($1/\tau_{LO}$) as in Fig. 6, plotted as a function of temperature for several different detection wavelengths.

through the phonon density and the electron distribution functions (the latter particularly because of the finite energy of the phonon). This mechanism is, therefore, crucially important in determining the temperature behavior of standard bound-continuum QWIPs and this is illustrated with the data in Fig. 6. The figure shows that for wavelengths greater than $10 \mu\text{m}$, the sequential tunneling is almost proportional to the temperature. Fig. 7 shows the same data but from the viewpoint of the effect of temperature on this contribution to the sequential-tunneling rate. It can be seen that for any given detection wavelength of a device, increasing the temperature from 77 to 300 K gives rise to an increase of approximately an order of magnitude in the electron-LO phonon sequential-tunneling contribution to the dark current.

V. CONCLUSION

A simple model for thermionic-emission-based and detailed quantum-mechanical calculations of both phonon and carrier-carrier scattering have shown that both the thermionic emission and sequential-tunneling contributions to the dark

current increase with increasing detection wavelength and increasing temperature for bound-to-continuum QWIPs. Both of these factors will make it difficult to extend the operating wavelength of conventional QWIPs to far-infrared (or terahertz) wavelengths.

The sequential-tunneling component to the dark current has been quantified, and for a fixed detection wavelength has been shown to be exponentially dependent on the width of the barriers between the QWs, with a decay constant in the range of $7\text{--}20 \text{ \AA}$. It is argued that this could be looked upon as a “dark current design rule.”

REFERENCES

- [1] E. Dupont, H. C. Liu, M. Buchanan, Z. R. Wasilewski, D. St-Germaine, and P. Chevette, “Pixel-less infrared imaging based on the integration of an n-type quantum well infrared photodetector with a light-emitting diode,” *Appl. Phys. Lett.*, vol. 75, p. 563, 1999.
- [2] H. Presting, M. Hepp, H. Kibbel, K. Thonke, R. Sauer, M. Mahlein, W. Cabanski, and M. Jaros, “Midinfrared silicon/germanium based photodetection,” *J. Vac. Sci. Technol. B*, vol. 16, p. 1520, 1998.
- [3] B. F. Levine, K. K. Choi, C. G. Bethea, J. Walker, and R. J. Malik, “Multiple quantum well $10 \mu\text{m}$ GaAs/Al_xGa_{1-x}As infrared detector with improved responsivity,” *Appl. Phys. Lett.*, vol. 50, p. 1814, 1987.
- [4] B. F. Levine, “Quantum well infrared photodetectors,” *J. Appl. Phys.*, vol. 74, p. R1, 1993.
- [5] S. Maimon, G. M. Cohen, E. Finkman, G. Bahir, D. Ritter, and S. E. Schacham, “Strain compensated ingaas/ingap quantum well infrared photodetector for mid-wavelength band detection,” *Appl. Phys. Lett.*, vol. 73, p. 800, 1998.
- [6] A. Foire, E. Rosencher, P. Bois, J. Nagle, and N. Laurent, “Strained ingaas/algaas quantum well infrared detectors at $4.5 \mu\text{m}$,” *Appl. Phys. Lett.*, vol. 64, p. 478, 1994.
- [7] B. F. Levine, C. G. Bethea, G. Hasnain, J. Walker, and R. J. Malik, “High detectivity $d^* = 1.0 \times 10^{10} \text{ cm}^2/\text{VHz}$ GaAs/AlGaAs multiquantum well $\lambda = 8.3 \mu\text{m}$ infrared detector,” *Appl. Phys. Lett.*, vol. 53, p. 296, 1988.
- [8] J. M. Chamberlain and R. E. Miles, Eds., *New Directions in Terahertz Technology*. Norwell, MA: Kluwer, 1997.
- [9] *Terahertz Spectroscopy and Applications—II*, vol. 3828, 1999.
- [10] D. Arnone, C. Ciesla, and M. Pepper, “Terahertz imaging comes into view,” *Phys. World*, vol. 13, no. 4, p. 35, 2000.
- [11] P. Harrison, *Quantum Wells, Wires and Dots: Theoretical and Computational Physics*. Chichester, U.K.: Wiley, 1999, p. 456.
- [12] S. D. Gunapala, J. K. Liu, J. S. Park, M. Sundaram, C. A. Shott, T. Hoelter, T.-L. Lin, S. T. Massie, P. D. Maker, R. E. Muller, and G. Sarusi, “ $9\text{-}\mu\text{m}$ cutoff 256×256 GaAs/Al_xGa_{1-x}As quantum well infrared photodetector hand-held camera,” *IEEE Trans. Electron Devices*, vol. 44, p. 51, 1997.
- [13] S. Gunapala, G. Surasi, J. Park, T. Lin, and B. F. Levine, “Infrared detectors reach new lengths,” *Phys. World*, vol. 7, p. 35, 1994.
- [14] H. C. Liu, A. G. Steele, M. Buchanan, and Z. R. Wasilewski, “Dark current in quantum well infrared photodetectors,” *J. Appl. Phys.*, vol. 73, p. 2029, 1993.

Nkaepe Etteh graduated from the University of Leeds, Leeds, U.K., in 1999, and is currently studying far-infrared (terahertz) QWIPs as part of the Ph.D. project.

Paul Harrison (SM’99) received the B.Sc. degree from the University of Hull, Hull, U.K., in 1988, and the Ph.D. degree from the University of Newcastle-upon-Tyne, Newcastle-upon-Tyne, U.K., in 1991.

He was a Postdoctoral Research Assistant at the University of Hull until 1995, when he obtained a Fellowship at the University of Leeds, Leeds, U.K. Since joining the Institute of Microwaves and Photonics, University of Leeds, he has been working on ways to adapt his theoretical and computational experience in semiconductor heterostructures to terahertz sources and detectors. He currently holds the position “Reader in Quantum Electronics.” He is author of the book *Quantum Wells, Wires and Dots* (Chichester, U.K.: Wiley, 1999).